Exoelectron emission during oxidation of Cs films

Cite as: J. Chem. Phys. **95**, 3756 (1991); https://doi.org/10.1063/1.460826
Submitted: 11 April 1991 • Accepted: 14 May 1991 • Published Online: 31 August 1998

A. Böttcher, R. Grobecker, R. Imbeck, et al.

Exoelectron emission during oxidation of Cs films

A. Böttcher, R. Grobecker, R. Imbeck, A. Morgante,[a] and G. Ertl
Fritz-Haber-Institut der Max-Planck-Gesellschaft, Faradayweg 4-6, W-1000 Berlin 33, Germany

(Received 11 April 1991; accepted 14 May 1991)

During oxidation of thin Cs films, a nonadiabatic surface reaction manifests itself in the emission of electrons. This effect was investigated in detail by combining measurements of the current and of energy distributions of these exoelectrons with studies on the electronic properties of the surface by means of ultraviolet photoelectron spectroscopy and metastable deexcitation spectroscopy. Exoelectron emission occurs via Auger deexcitation of the empty state derived from the O_2 affinity level. This process is confined to the stage $Cs_2O_2 \rightarrow CsO_2$ in which resonance ionization of the affinity level of the impinging O_2 molecule upon crossing the Fermi level E_F is efficiently suppressed due to the absence of metallic states near E_F. A kinetic model based on the successive steps involved in the oxidation of Cs is developed which describes qualitatively well all the experimental findings.

I. INTRODUCTION

The energy of an exothermic gas–surface reaction such as chemisorption or oxidation is usually released to the heat bath of the solid in the form of phonon excitations. The system can be considered to follow the adiabatic, electronic ground-state potential along the reaction coordinate. In the case of reactions between species with strongly differing electronegativities (such as an alkali-metal surface interacting with oxygen) the resulting bond will be highly ionic, and the adiabatic reaction path will be characterized by a crossing of the potential curve for $M + A$ with that for $M^+ + A^-$ as depicted schematically in Fig. 1 by a solid line circle. However, the impinging particle A may, in principle, avoid this charge transfer at the adiabatic crossing point and undergo this transformation only at a later stage on its way along the reaction coordinate. This process may be rationalized in terms of curve crossing of the $M + A$ potential with one of the electronically excited states of the $M^+ + A^-$ system. With metallic substrates the latter form a whole continuum of electron-hole pair excitations and the $M^+ + A^-$ ground-state potential is simply vertically displaced by the amount of this excitation energy.[1] Subsequent relaxation of the electron excitation may then occur either by phonon coupling (i.e., heat generation), or by photon and electron emission, respectively. The latter two processes of chemiluminescence and exoelectron emission are direct manifestations for the occurrence of nonadiabatic surface reactions, and several experimental observations of such effects have been reported so far in the literature.[2–14] In several of the quoted papers, the origin of exoelectron emission was sought in an Auger decay process, a concept which was corroborated by theoretical investigations.[1(b),15,16] However, the actual mechanism remained so far rather unclear. It was, for example, an open question why in oxidation reactions electron emission was not observed with clean surfaces but required preoxidation to a certain extent.[2–4] In the present work on the oxidation of Cs films the concerted application of various techniques led to clarification of this problem and to elucidation of the basic mechanism of electron emission as well as identification of competing processes. A first short report was published recently.[17] The present paper contains a full account of the experimental observations as well as their qualitative description within the framework of a kinetic model.

II. EXPERIMENT

The experiments were performed with an UHV system (base pressure of 10^{-10} mbar) which was equipped with a He discharge lamp for ultraviolet photoemission spectroscopy (UPS) ($h\nu = 21.2$ eV), an atomic beam source for metastable deexcitation spectroscopy (MDS), and a hemispherical electron energy analyzer for recording kinetic-energy distributions of electrons emitted from the surface. A detailed description of this apparatus has been published earlier.[18] Deexcitation of metastable noble-gas atoms A^* occurs at surfaces with low work function (such as Cs) via Auger deexcitation $A^* + T \rightarrow A + T^+ + e\ (E_{kin})$. The excitation energy of A^* (20.6 eV for ^1S He*, 19.8 eV for ^{3}He*) serves to emit an electron from the target whereby an energy balance analogous to UPS holds. In contrast to the latter technique, however, MDS is extremely surface sensitive and probes the valence electronic levels at a distance of a few angstroms from the surface[19,20]—just as do the impinging O_2 molecules whose chemical interaction gives rise to exoelectron emission.

Polycrystalline films of Cs with varying thickness were formed by evaporation from a SAES getter source onto a clean Ru(001) surface, which was typically kept at 220 K. Relative thicknesses of the films were derived from integrating the Cs thermal-desorption spectroscopy (TDS) traces recorded by means of a quadrupole mass spectrometer.[21] Calibration was achieved through the monolayer capacity (1 ML) which for Cs/Ru(001) is characterized by a $\sqrt{3} \times \sqrt{3}$ R 30° low-energy electron-diffraction (LEED) pattern and corresponds to a density of 5.3×10^{14} Cs atoms/cm^2.[22,23]

The work function ϕ and its changes were determined from the total width w on the energy scale of the ultraviolet photoelectron spectra, since $h\nu = w + \phi$. The total current of exoelectrons emitted from the sample surface was recorded by means of a Faraday cup device. Because of their low work functions, these systems are photocathodes of high

[a] A. von Humboldt Fellow. Present address: Laboratorio Technologie Avanzate Superfici e Catalisi, Padriciano 99, I-24012 Trieste, Italy.

 0021-9606/91/173756-11$03.00

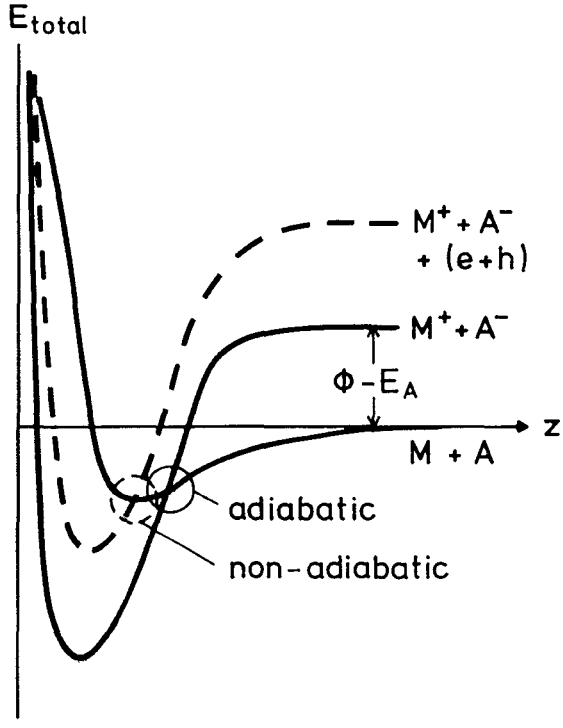

FIG. 1. Schematic potential diagram illustrating the possibility of electronic excitation accompanying the interaction between reactants of differing electronegativities, such as Cs(M) + O_2 (A).

sensitivity and hence extreme care had to be taken to suppress any spurious electron emission caused by external light sources.

III. RESULTS

The interaction of O_2 with Cs films under conditions comparable to those applied in the present work had been studied in detail before.[24] Oxidation proceeds through various stages: At first suboxides containing the structural unit $Cs_{11}O_3$ are formed. In these the O^{2-} ions are incorporated below the surface which itself remains in its zerovalent state as characterized by the presence of filled Cs 6s levels just below the Fermi level E_F. Next, a continuous transformation into the peroxide, Cs_2O_2, takes place in which all Cs atoms are ionic and oxygen is present as O_2^{2-} ions. The work function reaches a minimum around completion of this stage and continuously increases upon further oxygen exposure, concurrently with the formation of the hyperoxide species, CsO_2, containing O_2^- ions.

The interference of surface and bulk oxidation processes becomes evident if the variation of the work function with oxygen exposures for Cs films of varying thickness is recorded. The larger the latter, the higher is the O_2 exposure required to reach the ϕ minimum as well as the final level. With thicker films frequently not a single minimum is observed, and the shape of the curve becomes sensitively affected by the temperature as well as by the rate of adsorption (equal to the O_2 pressure) and mode of exposure. These effects reflect the superposition of surface effects and of bulk oxidation limited by the mobility of Cs atoms. In order to rationalize the experimental findings, the main part of results to be presented will hence be restricted to experiments with relatively thin (<4 ML) Cs films.

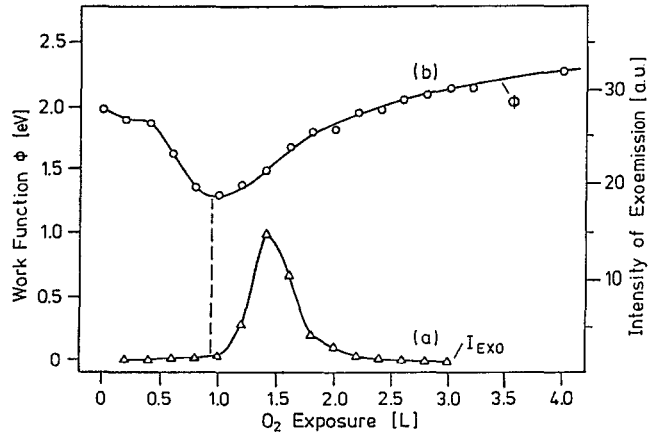

FIG. 2. Variation of the current of exoelectrons [in arbitrary units, curve (a)] and of the work function ϕ [curve (b)] upon stepwise exposure of a Cs film with about 3 ML thickness at 220 K to an O_2 pressure of 4×10^{-9} mbar.

As a typical example, Fig. 2 shows the work-function variation with (stepwise) O_2 exposure [curve (b)] with the concurrently recorded total current of exoelectron emission [curve (a)]. More specifically, the sample was exposed to 4×10^{-9} mbar O_2 for a certain time interval during which the energy distribution of the emitted exoelectrons was recorded, and the (relative) yield of exoelectrons was derived from integration of this energy distribution curve. The first 0.3 L (1 L = 10^{-6} Torr s) exposure of O_2 cause almost no change of the work function due to bulk diffusion of the O atoms. The length of this plateau depends on the thickness of the Cs film as well as on the dosing conditions. Then, the work function drops due to the formation of $Cs_{11}O_3$ units at the surface. Clearly, a clean Cs surface is totally inactive towards electron emission, although the largest amount of energy is released in the initial step of oxidation to $Cs_{11}O_3$. Qualitatively, similar observations were made in previous studies with Mg surfaces.[3,4] In the latter case it was suggested that the electron yield would increase with decreasing work function.[11] Although this effect will be of importance, as demonstrated below, it certainly will not be decisive. The data of Fig. 2 demonstrate that the electron yield reaches in fact its maximum only *beyond* the ϕ minimum. Thus we have to conclude that electron emission is essentially confined to the stage of the surface where the work function rises again, i.e., to the range of the transformation $Cs_2O_2 \rightarrow CsO_2$ at the surface. This suggests that it is primarily the chemical state, i.e., the valence electronic structure, at the surface which governs the efficiency of the nonadiabatic reaction branch.

In order to substantiate this idea further, the electronic structure of the outer surface was probed by MDS parallel to recording the yield of exoelectrons. Figure 3 shows a set of data from the energy range close to the Fermi level recorded with ^1S He* from a Cs film after various O_2 doses. (Note that this film was thinner than that one underlying the data of Fig. 2. Hence the onset of exoelectron emission occurs at a lower oxygen exposure and the initial work function plateau is almost absent.) The impinging singlet He* atoms are

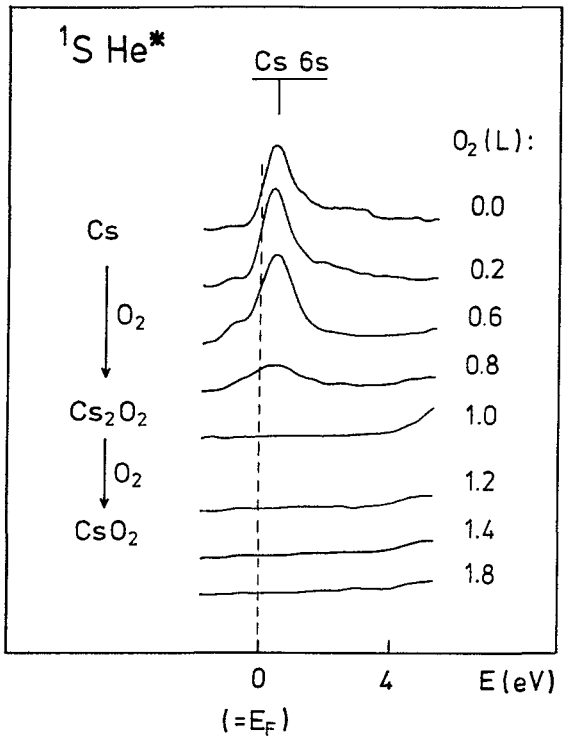

FIG. 3. Metastable deexcitation spectroscopy (MDS) from the valence-band region of a thin Cs film with increasing O_2 exposure. (Most of the impinging singlet He* atoms are converted into the triplet state and the dashed line marks E_F for deexcitation of ^3S He*. The small contributions above E_F arise from residual ^1S He* deexcitation.)

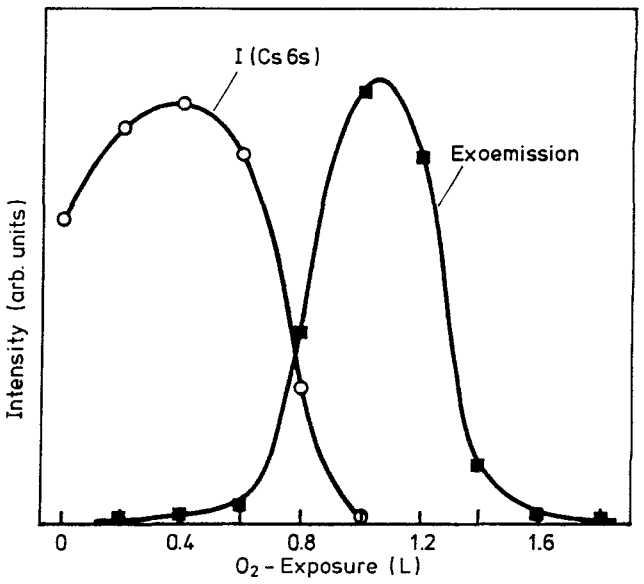

FIG. 4. Variation of the MDS intensity from the Cs 6*s* emission and of the exoelectron current with O_2 exposure.

largely converted into triplet species (with 0.8 eV lower excitation energy) prior to complete deexcitation,[24,25] and hence the energy zero ($= E_F$) is set equal to the onset of ^3S He* emission. The spectrum from the clean Cs surface is characterized by a pronounced peak just below E_F due to emission from the occupied Cs 6*s* bands.[20,24] (The weak feature above E_F arises from the small fraction of impinging He* atoms which had not undergone the singlet-to-triplet conversion.) Upon admission of O_2 the intensity of this peak at first even increases, although the formation of the O^{2-} ions (in $Cs_{11}O_3$) consumes part of the Cs 6*s* electrons. This phenomenon was investigated earlier and was interpreted in terms of a quantum-size effect:[26] The negatively charged oxygen ions in the $Cs_{11}O_3$ building block repel the remaining Cs 6*s* valence electrons, whereby these become more restricted in space and rise in kinetic energy—hence the work function is lowered and the wave functions "leak" further out of the surface where they are probed by the He* atoms.

Further oxidation then leads to the formation of Cs_2O_2 consisting of O_2^{2-} and Cs^+ ions (and in parallel already to the onset of CsO_2 formation), and therefore now the intensity of Cs 6*s* emission decreases. Figure 4 shows that the yield of exoelectrons is low as long as the Cs 6*s* intensity is high; it rises when the latter drops, i.e., when the density of occupied states just below the Fermi level is depleted. The exoelectron emission takes place with maximum efficiency after the Cs 6*s* intensity dropped to zero (i.e., the surface exposes merely Cs^+ ions); its decrease at even higher oxygen exposures is strongly affected by the continuous rise of the work function as will be shown later.

Although these observations strongly indicate that exoelectron emission is essentially confined to the stage

$$Cs_2O_2 \xrightarrow{O_2} CsO_2,$$

for energetic reasons it cannot be simply this reaction which gives rise to electron emission: The reaction $Cs_2O_2 + O_2 \rightarrow 2CsO_2$ is exothermic only by ~ 1.0 eV,[27] while for an electronic excitation from the Fermi level at least 1.5 eV would be necessary in order to overcome the work-function barrier. (The maximum energy of excited electrons is even higher, namely about 2.7 eV, as will be shown below.) It turns out that, although metallic Cs atoms in the outermost layer are prohibitive for exoelectron emission, their presence in the subsurface region is a necessary requirement: UPS probes the electronic properties not only of the outer surface but of a layer of about 5–10 Å thickness. As long as Cs is in its zero valent state its $5p_{3/2}$ and $5p_{1/2}$ levels are located at 12.1 and 14.0 eV binding energy, respectively, while these are shifted to 11.5 and 13.5 eV upon transformation into Cs^+ upon oxidation. It turned out that in the exposure range over which exoelectron emission was observed the UPS data still exhibited contributions from Cs^0 species (although these were absent on the surface). More specifically, the presence of Cs^0 as a constituent of the $Cs_{11}O_3$ building unit of the cesium suboxides can be monitored by probing the existence of the octahedrally coordinated O^{2-} ions which are characterized in UPS by a 2*p*-derived peak at $E_B = 2.8$ eV.[24,28,29] UPS data from this energy range taken after successive oxygen exposures show the growth and decay in intensity of this peak assigned to O^{2-} species (no corresponding peak is seen in MDS, signaling the presence of this species below the surface). Interestingly, exoelectron emission with high efficiency is observed mainly

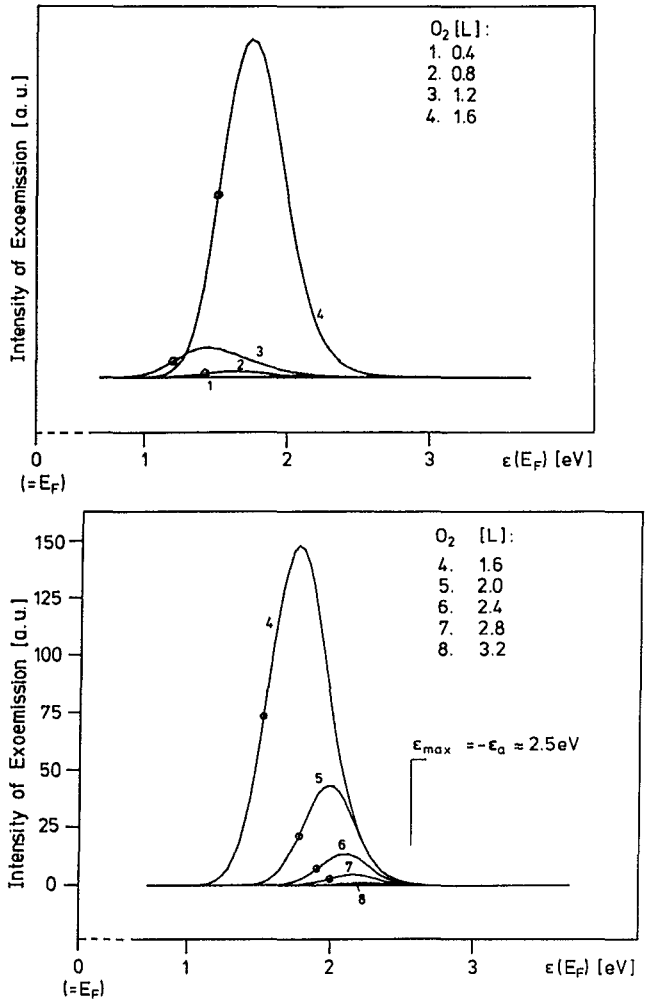

FIG. 5. Kinetic-energy distributions (with respect to the Fermi level E_F) of exoelectrons emitted at various stages of oxidation. Circles mark the respective value of the work-function cutoff. (a) Data for O_2 exposures below the maximum of exoemission (see Fig. 2). (b) Data for O_2 exposures above I_{max}.

just within that range of oxygen exposures over which O^{2-} ions (accompanied by Cs^0 in $Cs_{11}O_3$ units) are present in the subsurface region.

Figure 5 displays a series of energy distributions of the emitted exoelectrons as recorded with the hemispherical electron energy analyzer at a relatively poor resolution (for sensitivity reasons) of 0.3 eV. The scale of kinetic energies refers to the Fermi level, and the open circles mark the cutoffs as determined by the corresponding work functions. For the sake of clarity, data for O_2 exposures below that for the exoemission intensity maximum are displayed in Fig. 5(a), and those beyond this maximum in Fig. 5(b). At the work-function minimum the energy distribution has the lowest cutoff (curve 3) which then shifts to higher energies while simultaneously the integral intensity rises. This demonstrates again clearly that the maximum yield of exoelectrons does not coincide with the work-function minimum. Further increase of the O_2 exposure beyond that necessary for the maximum electron yield leads to energy distributions with continuously shifting cutoff (due to the continuous work-function rise) which exhibit at first a common leading edge. Only at even higher exposures also the intensity at the high-energy edge drops. The maximum kinetic energy with respect to the Fermi level lies at about 2.5 eV.

Figure 6 shows how for Cs films of the same thickness the current of exoelectron emission varies as a function of time with O_2 pressure. The time t_{max} after which the maximum emission intensity I_{max} is reached varies approximately proportional to $1/p_{O_2}$, or in other words, is reached roughly after the same exposure $\int p_{O_2}\, dt$. This suggests that exoemission is a first-order rate process with respect to p_{O_2}. Extrapolation to atmospheric pressure yields an I_{max} at about 2×10^{-9} s! (Of course, it will not be possible to realize an adequate pressure jump within such a short period of time.)

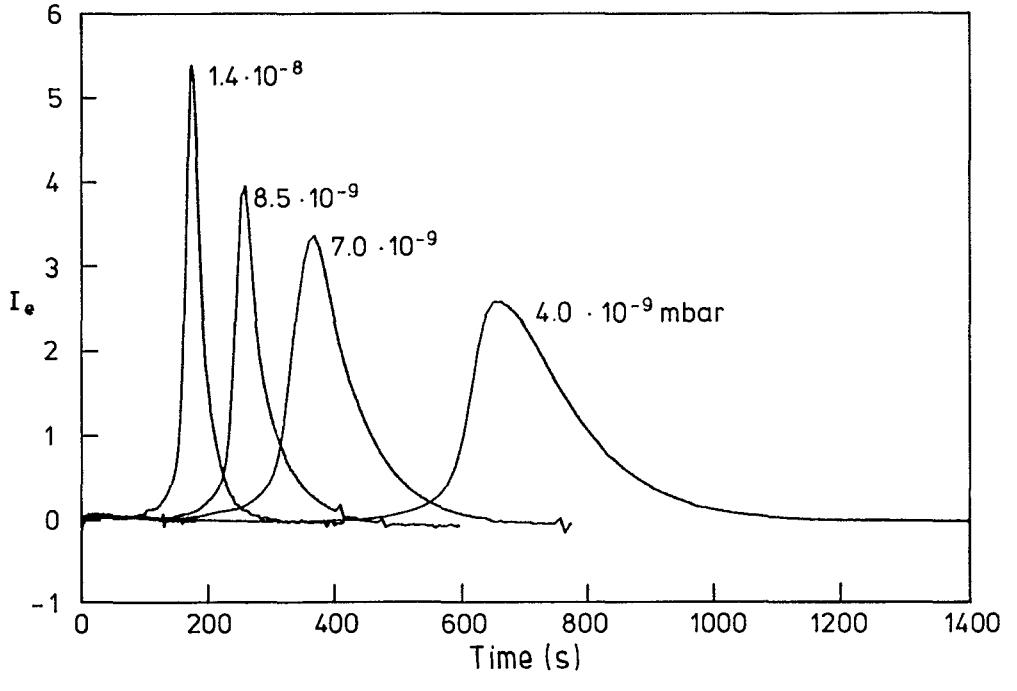

FIG. 6. Variation of the exoelectron current with time at various O_2 pressures for Cs films with the same thickness of 3.4 ML, and at the same temperature $T = 190$ K.

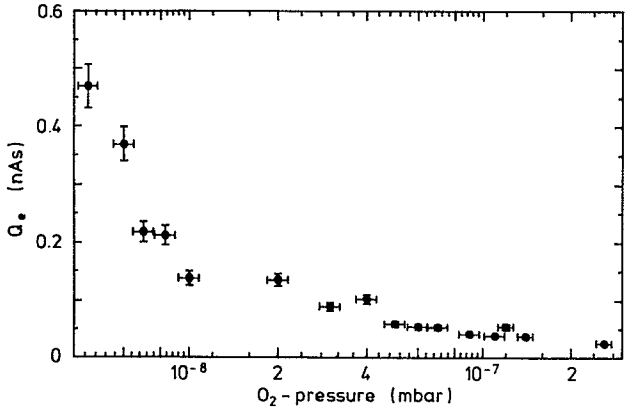

FIG. 7. Variation of the total exoelectron charge Q_e associated with complete oxidation of Cs films of 3.4 ML thickness with the O_2 pressure applied during (continuous) exposure.

During O_2 exposure and recording of the exoelectron current the ionization gauge as well as the quadrupole mass filter had to be switched off in order to avoid any spurious effects due to photoemission from the low work-function surfaces caused by the hot filaments. As a consequence p_{O_2} drifted somewhat, in particular during the long exposure times required at the lowest pressures, and hence the fairly large fluctuations in the product $t_{max} \cdot p_{O_2}$ This effect is, however, without relevance for determination of the total yield of exoelectrons, $Q_e = \int I\,dt$. Quite surprisingly, this quantity was found to apparently depend on pressure, or, more specifically, to decay with p_{O_2} as shown in Fig. 7. This dependence is nearly of the form $Q_e \sim 1/p_{O_2}$, so that a very small total yield would result from an extrapolation to atmospheric pressure. At $p_{O_2} = 10^{-8}$ mbar the mean free path in the gas phase is so large that collisions between O_2 molecules can be completely neglected. On the other hand, it will take about 100 s until the same site, *on the average*, will be hit again by an O_2 molecule from the gas phase. Any elementary steps requiring multiple collisions by O_2 (as at first suggested by this effect) can therefore certainly be excluded. The solution of this puzzle was found with a series of experiments in which the surface was not exposed to a *constant* p_{O_2}, but to pulses of the same pressure interrupted by intervals of varying length. The resulting data are reproduced in Fig. 8. It turns out that, *for the same* p_{O_2} *and pulse lengths* τ, the exoelectron yield increases with the time of interruption of the gas flow, Δt. In addition and more specifically, I_{max} is reached for $\Delta t = 20$ s during the first pulse, for $\Delta t = 40$–80 s during the second pulse, and for $\Delta t = 110$ s only at the third pulse. This result indicates that it is in fact not the O_2 pressure, but the duration of exposure (which becomes longer if p_{O_2} is smaller) which determines the yield of exoelectrons, or, in other words, there has to be a competing process involved which is independent of p_{O_2}.

As a further surprise, the total yield of exoelectron emission was found to depend sensitively on the substrate temperature, too. As can be seen from Fig. 9(a), it increases considerably with temperature between 177 and 244 K, while the O_2 exposure at which I_{max} is reached is essentially independent of T. The latter finding suggests that the oxygen sticking coefficient is in fact not appreciably temperature dependent in this range. Figure 9(b) shows a plot of log Q_e vs $1/T$, and from the resulting straight line an apparent activation energy of 11.5 kJ is derived. The pronounced variation of the yield with temperature suggests competition of the reaction step leading to electron emission with another process in which the electronic excitation is quenched, whereby at least one of these two parallel reactions is thermally activated.

If we consider the data for $T = 244$ K, a total charge of 3.43×10^{-10} As ($\approx 2 \times 10^9$ electrons) was emitted by oxidation of about 0.3 cm^2 of Cs with 3 ML thickness to CsO_2, thus corresponding to the uptake of 0.5×10^{15} O_2 molecules. From this we estimate that the efficiency of a reacting O_2 molecule in emitting an electron is of the order 10^{-5}–10^{-6} at the applied pressure of 10^{-8} mbar. This efficiency might

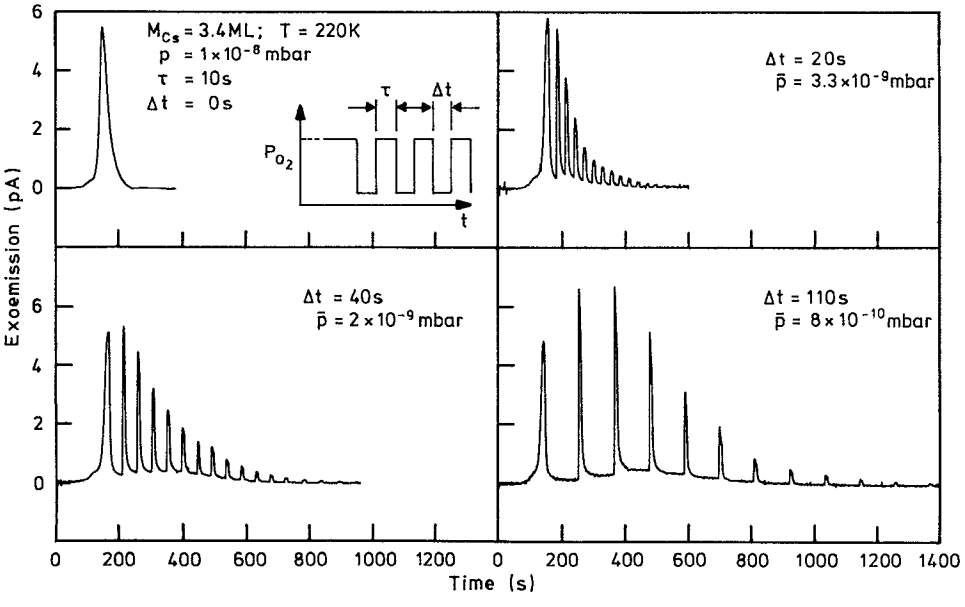

FIG. 8. Exoelectron currents as a function of time from Cs films of 3.4 ML thickness which were exposed to 1×10^{-8} mbar O_2 for $\tau = 10$ s with varying times of interruption Δt. p denotes the *average* partial pressure which would result if the total particle flux is divided by the total time of exposure. (a) $\Delta t = 0$ s, i.e., continuous exposure to $p = 10^{-8}$ mbar. (b) $\Delta t = 20$ s, $p = 3.3 \times 10^{-9}$ mbar. (c) $\Delta t = 40$ s, $p = 2 \times 10^{-9}$ mbar. (d) $\Delta t = 110$ s, $p = 8 \times 10^{-10}$ mbar.

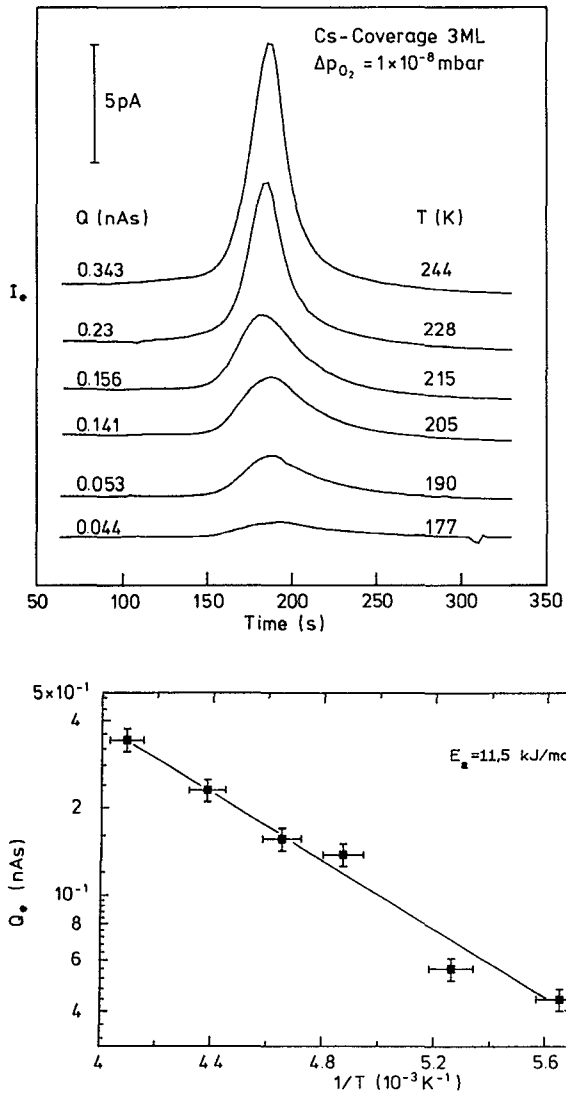

FIG. 9. (a) Exoelectron current as a function of time for exposure of 3 ML thick Cs films to 10^{-8} mbar O_2 at various temperatures. (b) Plot of log Q_e of the previous data vs $1/T$.

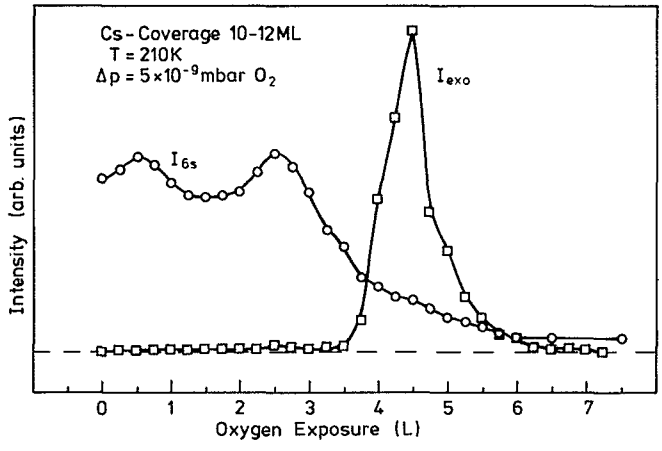

FIG. 10. Variation of the Cs 6*s* intensity in MDS, I_{6s}, and of the exoelectron current, I_{exo}, with oxygen exposure of a 12 ML thick Cs film.

be increased by probably up to one order of magnitude if exposure is made at even lower pressures (cf. Fig. 8), while higher temperatures are not feasible due to the onset of evaporation of Cs.

The superposition of surface and bulk oxidation effects, as already mentioned above in connection with the variation of the work function with O_2 exposure, manifests itself also with the MDS data and with the exoelectron emission characteristics. Figure 10 shows results for a Cs film with about

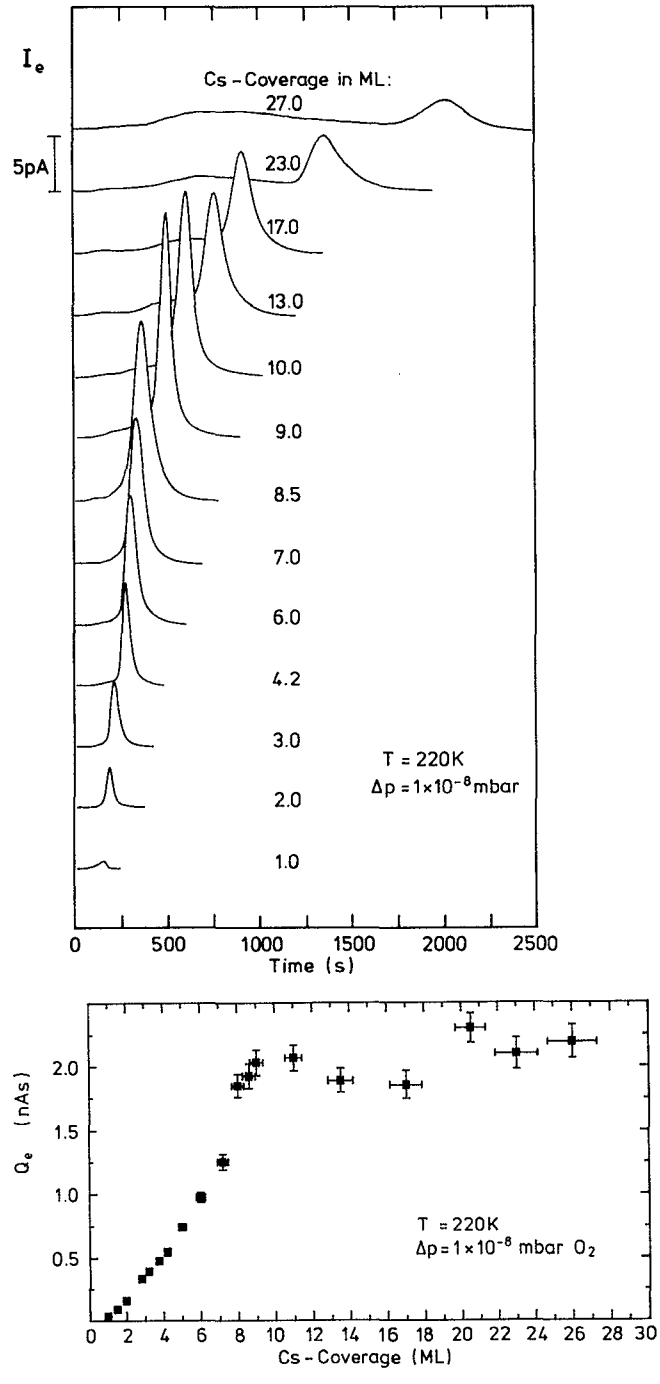

FIG. 11. (a) Exoelectron current as a function of time upon exposure of Cs films with varying thickness to 1×10^{-8} mbar O_2 at 220 K. (b) Total yield of exoelectrons upon oxidation of Cs films with varying thickness.

12 ML thickness. The decay of the Cs intensity in MDS and the rise of exoelectron emission have their onset only after about 3 L O_2 exposure, and again the current of exoelectron emission appears at a stage at which the 6*s* intensity has strongly decreased (but still is finite, in contrast to Fig. 2 for a thin film).

As can be seen from Fig. 11(a), the time t_{max} for reaching the maximum exoelectron current shifts to higher values with increasing thickness of the Cs film while also multiple maxima occur. The total yield of exoelectrons [Fig. 11(b)] increases with the thickness of the Cs layer up to about 10 ML and then levels off. This result indicates again that exoemission is associated with progressing oxidation involving bulk diffusion; the latter process eventually becomes so slow that the exoelectron yield does not increase any more with even further increase of the film thickness.

The regular (bulk) cesium oxides are no longer formed if this element is only present in quantities below a monolayer. Nevertheless, small yields of exoelectrons can still be observed. Such systems are presently under detailed investigation and will be treated elsewhere.[30]

IV. DISCUSSION

For discussion of the mechanism of exoelectron emission with the present system we adopt a model first proposed by Nørskov, Newns, and Lundqvist[16] for surface chemiluminescence, and later extended by the same group,[1(b),15] as well as by others,[11,14] to the case of reactive electron emission. The basic idea is illustrated by Fig. 12(a): When an O_2 molecule approaches the Cs surface its electron affinity level

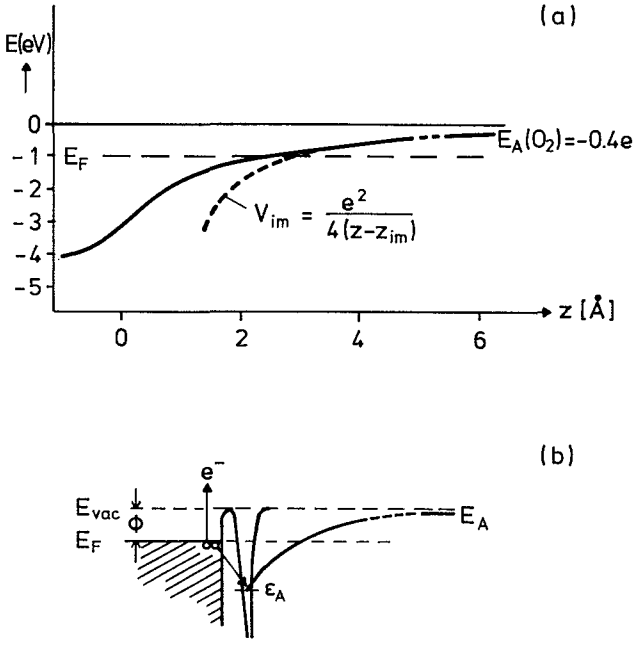

FIG. 12. (a) Schematic variation of the energy of the affinity level of O_2 with distance from a metal surface. (b) Mechanism of Auger deexcitation of the state ϵ_A derived from the O_2 affinity level eventually leading to exoelectron emission.

(which for the free molecule is about 0.4 eV below the vacuum level) will first be lowered due to image force effects and then closer to the surface even more by the onset of chemical bond formation (which eventually may also lead to dissociation and creation of anions). The final combined system will exhibit a series of O 2*p*-derived levels presented in Fig. 12(b) schematically by ϵ_A. In the adiabatic limit, the incoming particle will be resonance ionized as soon as E_A crosses the Fermi level. (This corresponds to the adiabatic curve crossing of the potential curves representing the total energy in Fig. 1.) Due to the nonvanishing velocity of the nuclear motion there might, however, be a finite probability that the O_2 molecule reaches the surface without E_A being filled. Although there is then still the possibility of resonance ionization via degenerate states from the substrate, there exists also a channel for nonadiabatic deexcitation via an Auger process as indicated in Fig. 12(b), leading to electron-hole pair excitation in the solid. The maximum energy of the excited electron (with respect to the Fermi level) will be given by $E_{max}(E_F) = -E_A$. Only those electrons whose excitation energy exceeds the work function ϕ may escape into the vacuum and contribute to the exoelectron current.

Since exoemission was found to be confined to the stage $Cs_2O_2 \rightarrow CsO_2$ during which no dissociation of the reacting O_2 molecules occurs, the presented picture will not be complicated by bond-breaking processes (such as inferred with other systems[11,14-16]), and we identify ϵ_A with the highest-lying O_2-derived level in the Cs_2O_2/CsO_2 system. This state is probed by UPS at 3.3 eV below E_F, and shifts with increasing oxygen exposure to 2.4 eV;[24] this value corresponds nicely with the observed maximum kinetic energy of the emitted exoelectrons (with respect to E_F) of about 2.5 eV (see Fig. 5). The minimum kinetic energy (again with respect to E_F) of the emitted electrons will, on the other hand, be determined by the work function, and the cutoff of the energy distributions reproduced in Fig. 5 follows indeed the variation of ϕ. This explains also why the *total* yield of *emitted* electrons will be strongly dependent on the work function, even if their *excitation* probability remains constant. (Prince, Lambert, and Foord[11] concluded that this dependence should approximately follow a third power law with respect to ϕ.) Such a situation is found with the data of Fig. 5(b) showing a common leading edge of their high E_{kin} tail, while the rising work function prevents lower-energy electrons more and more from escaping from the surface. This is the primary reason for the decrease of the exoemission current just beyond its maximum, while at even higher O_2 exposures "chemical" saturation terminates this process.

While the total efficiency for electron *emission* is fairly low (of the order 10^{-6} as outlined above), the probability of electronic *excitation* is indeed much higher.

At a certain stage of oxidation, a nonadiabatic reaction is hence in fact more than a spurious effect. Why?

The probability of the incoming particle to "survive" resonance ionization upon crossing of its affinity level with the Fermi level will be governed by the lifetime τ_{el} of this hole state. The latter is inversely proportional to the level width, which in turn is determined by the coupling matrix element $V_{ak} = \langle a|H_e|k\rangle$ between the one-electron states of

the substrate $|k\rangle$ and of the adsorbate $\langle a|$,[1(b)] and hence it is governed by the overlap between the wave functions of the empty affinity level of the impinging particle and of occupied states of the surface near E_F. As long as the impinging O_2 molecule "sees" occupied 6*s* levels of Cs^0 atoms (such as probed by the He* particles in MDS) the electronic transition will take place much more rapidly than nuclear motion (equal to Born–Oppenheimer) and the reaction follows the adiabatic path. If, on the other hand, the oxygen strikes a site which has already been transformed into Cs^+ ($=Cs_2O_2$), τ_{el} will become long enough to permit electronic excitation. This picture is supported by the data of Fig. 4 which show that the exoemission current rises when the Cs 6*s* intensity as probed by MDS decays. The Auger deexcitation process actually leading to exoelectron emission as depicted schematically in Fig. 12, on the other hand, still requires electrons from close to the Fermi level. It is suggested that these are delivered by the Cs^0 atoms "buried" below the surface as signaled by the concurrently present O^{2-} ions probed by UPS. This process will *not* depend on p_{O_2} and will compete with the oxidation step $Cs_2O_2 + O_2 \rightarrow 2CsO_2$ whose exothermicity will not be sufficient for electron emission. Both competing processes are expected to be thermally activated in a different manner, and in this way it becomes plausible why the total yield of exoelectrons is dependent on temperature. The manifestation of the superposition of surface and bulk processes has already been emphasized at various other points.

Based on the conclusions presented, a simple kinetic scheme will now be developed for more detailed modeling of the observed phenomena. This scheme starts from the following input information.

(a) The first O_2 molecules impinging on a fresh Cs film penetrate, after dissociation at the surface, into the bulk without affecting markedly the surface properties (cf., for example, the variation of the work function in Fig. 2). This effect is modeled by assuming a thickness-dependent "dead" initial exposure.

(b) Oxidation of the surface region occurs via

$$Cs \xrightarrow{O_2} Cs_{11}O_3 \xrightarrow{O_2} Cs_2O_2 \xrightarrow{O_2} CsO_2.$$

The respective surface concentrations are denoted by $x_1 = [(Cs)]$, $x_2 = [Cs_{11}O_3]$, $x_3 = [Cs_2O_2]$, and $x_4 = [CsO_2]$. For the sake of simplicity, it is assumed that these are the only surface species (i.e., the presence of O_{ad}, for example, is neglected), and the sum of surface concentrations is constant and normalized, $\Sigma x_i = 1$.

(c) The intensity of the Cs 6*s* peak probed by MDS, I_{6s}, increases at first with oxygen exposure (due to the mentioned quantum-size effect), and then decreases due to complete ionization of the Cs atoms.

A plausible ansatz is

$$I_{6s} = x_1 I_{Cs} + x_2 I_{Cs_{11}O_3} = i_0 (x_1 + \alpha x_2),$$

whereby I_{Cs} and $I_{Cs_{11}O_3}$ are the intensities from pure Cs and $Cs_{11}O_3$ surfaces, respectively. From experimental data $\alpha \approx 1.5$ is derived.

(d) The work function ϕ at first decreases, reaches a minimum around the stage where the surface has been completely transformed into Cs_2O_2, and then increases again. Its value is modeled by a similar ansatz

$$\phi = x_1 \phi_{Cs} + x_2 \phi_{Cs_{11}O_3} + x_3 \phi_{Cs_2O_2} + x_4 \phi_{CsO_2},$$

whereby the following parameters were used: $\phi_{Cs} = 2.1$ eV (equal to the clean surface), $\phi_{Cs_{11}O_3} = 1.2$ eV, $\phi_{Cs_2O_2} = 1.0$ eV and $\phi_{CsO_2} = 2.2$ eV (equal to the final value).

(e) Exoelectron emission is restricted to the stage $Cs_2O_2 \rightarrow CsO_2$. More specifically, it is assumed that the final stage of oxidation into CsO_2 occurs via two competing steps from which only one will lead to electronic excitation eventually followed by exoelectron emission:

(i) Direct transformation of a Cs_2O_2 site will occur without electron emission, *inter alia* because of insufficient exothermicity (see above).

(ii) Diffusion of a zero valent Cs atom from below the surface near a Cs_2O_2 site will provide the occupied electron levels near E_F required for the Auger deexcitation process leading to electronic excitation as discussed above. This rate process will be activated, but not dependent on p_{O_2}. In this way the data of Figs. 7–11 will find a plausible explanation. Schematically, this branching reaction may be formulated as

$$\begin{array}{l} Cs_2O_2 + O_2 \xrightarrow{k_4} CsO_2 \\ \downarrow k_3 \\ Cs_2O_2^* \end{array}$$

and electronic excitation will require the presence of the $Cs_2O_2^*$ surface species. We therefore split up the surface concentration of Cs_2O_2 into x_3' from the "normal" species and x_3'' denoting the $Cs_2O_2^*$ species, whereby the latter might, in principle, also be of different chemical origin, i.e., $x_3 = x_3' + x_3''$. However, there would still be no chance for Auger deexcitation if the incoming O_2 molecule would not be efficiently shielded from resonance ionization. As a rough approximation it is hence assumed that the sites which are active for exoemission are composed of a $Cs_2O_2^*$ unit which is neighbored by two CsO_2 entities, i.e., the probability is proportional to x_4^2. (If only one CsO_2 neighbor were assumed the results would not be affected qualitatively.) A pure $Cs_2O_2^*$ site without "isolating" neighbors on the surface, on the other hand, would presumably be directly converted with high probability into CsO_2 without electron excitation.

The probability for excitation of electron-hole pairs is then given by

$$P_e = k_e \cdot p_{O_2} \cdot x_3'' \cdot x_4^2.$$

(f) As shown in detail, only a small fraction of the excited electrons will be able to escape from the solid and contribute to the exoelectron current because of the work-function barrier, hence

$$I_{exo} = P_e \cdot f(\phi).$$

To a first approximation, $f(\phi)$ will vary roughly inversely proportional to ϕ. More specifically, the following approximate dependence derived by Prince, Lambert, and Foord[11]

was used for the analysis

$$f(\phi) \sim (E_A - \phi)^3,$$

and hence $I_{exo} = k_e \cdot p_{O_2} \cdot x_3'' \cdot x_4^2 \cdot f(\phi)$.

The following kinetic equations are based on the mentioned sequence of reaction steps and neglect any differences in stoichiometric factors (which can be thought of being incorporated in the rate constants) as well as in the specific area occupied by the various species on the surfaces:

$$\frac{dx_1}{dt} = -k_1 p_{O_2} x_1,$$

$$\frac{dx_2}{dt} = k_1 p_{O_2} x_1 - k_2 x_2 p_{O_2},$$

$$\frac{dx_3'}{dt} = k_2 p_{O_2} x_2 - k_3 x_3' - k_4 p_{O_2} x_3',$$

$$\frac{dx_3''}{dt} = k_3 x_3' - k_e p_{O_2} \cdot x_3'',$$

$$\frac{dx_4}{dt} = k_e p_{O_2} \cdot x_3'' + k_4 p_{O_2} x_3'.$$

This set of coupled differential equations was solved numerically by the use of properly chosen parameters (as indicated in the figure captions) for the variation of the concentrations of the various surface species with time after switching on a fixed p_{O_2} at $t = t_1$, whereby t_1 denotes the above-mentioned "dead" time.

A series of typical results is reproduced in Fig. 13: Figure 13(a) shows the variation of the concentrations x_i, and Fig. 13(b) displays the experimentally observable quantities ϕ, I_{6s}, and I_{exo} which are to be compared with the actual measurements reproduced, e.g., in Figs. 2 and 3(b). Obviously, all essential features are qualitatively reproduced, in particular, the fact that I_{exo} reaches its maximum only beyond the ϕ minimum at a stage at which I_{6s} has already largely decayed.

For comparison with Fig. 6, Fig. 14 shows how the calculated variation of I_{exo} with time depends on the O_2 pressure. The observed decrease of t_{max} and increase of i_{max} with increasing p_{O_2} is again clearly reproduced. In addition, the totally emitted charge $Q_e = \int I_{exo}\, dt$ decreases with increasing p_{O_2}, in qualitative agreement with the experimental data of Fig. 7.

Within the presented model the fact that the excitation probability P_e (i.e., the probability for nonadiabatic reaction) never reaches 100%, even under optimum conditions, is attributed to the competition between the two parallel reaction steps for transformation of the Cs_2O_2 species with the rate constants k_3 and k_4, which also accounts for the observed temperature dependence of the total exoelectron yield. More specifically, the apparent activation as derived in Fig. 9(b) reflects, within this model, the difference in the activation energies of the rate constants k_3 and k_4. This, on the other hand, indicates that the elementary step leading to Auger deexcitation is actually coupled to a thermally activated process (such as presumably diffusion of Cs^0 from below the surface which provides the electrons from near E_F).

The fact that one of these steps (k_4) comprises further oxidation of Cs_2O_2 and hence depends on p_{O_2}, while the other one (k_3) depends only on time, but not on oxygen pressure, was deduced from the experiments depicted in Fig. 8 in which the same p_{O_2} was applied with interruptions of varying interval lengths. Again, these data are qualitatively reproduced by the model presented. As can be seen from Fig. 15, the maximum current (and also the total charge emit-

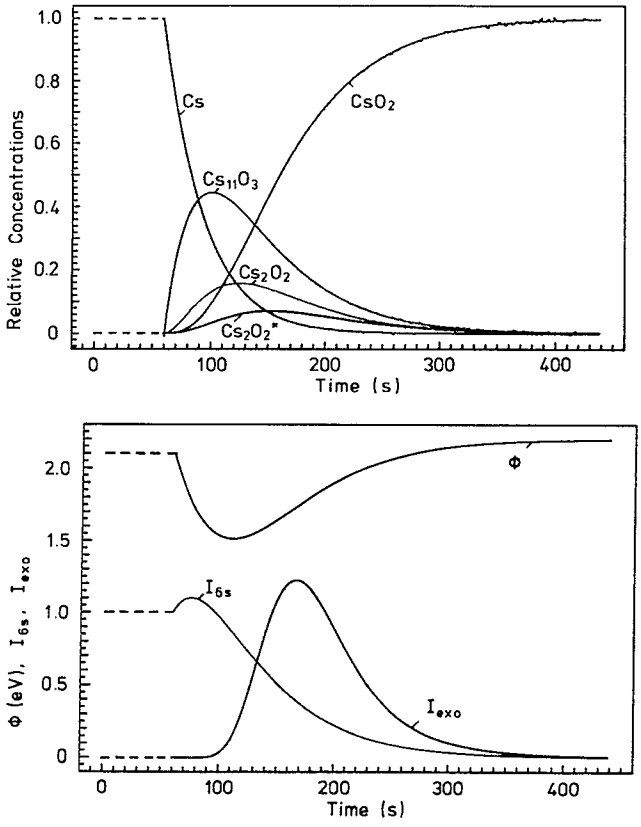

FIG. 13. Temporal evolution of the system described by the kinetic model using the following parameters: $t_1 = 60$ s; $k_1 = 9$, $k_2 = 6$, $k_3 = 6$, $k_4 = 9$, $k_e = 12$ (in units of 10^{-17} cm^2, corresponding to $p_{O_2} = 10^{-8}$ mbar). (a) Variation of the concentrations x_i of the various surface species with time. (b) Variation of the work function ϕ of the Cs 6s intensity in MDS, I_{6s}, and of the exoelectron current, I_{exo}, with time.

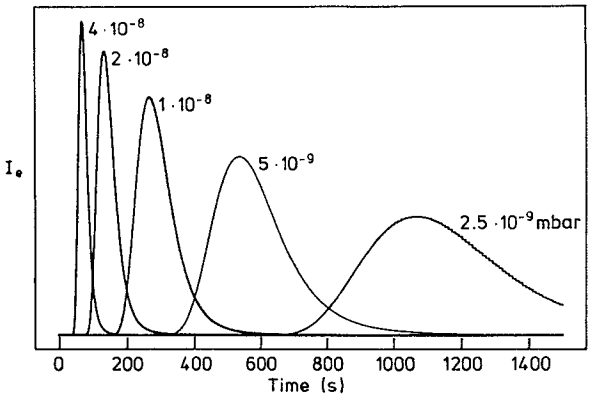

FIG. 14. The effect of O_2 pressure on the temporal evolution of I_{exo} as evaluated from the kinetic model.

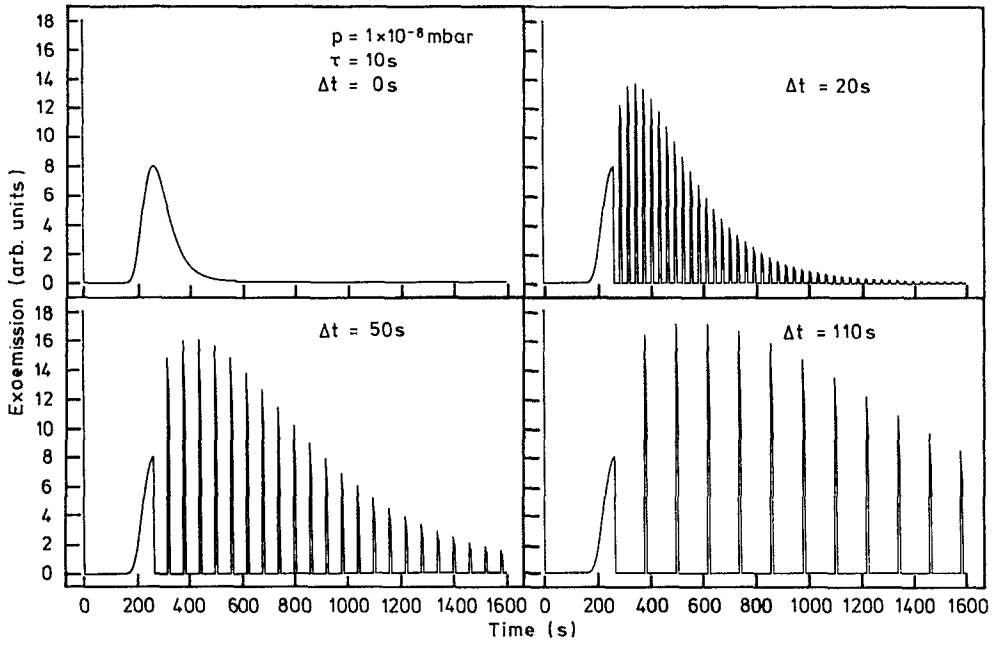

FIG. 15. Modeling of the experiments with interrupted gas dosage (cf. Fig. 8) as evaluated from the kinetic model.

ted) increases with increasing duration of interruption Δt of the oxygen exposure at fixed pressure. (The tails of the spikes in the actual experimental data of Fig. 8 can easily be reproduced if the noninstantaneous drop of the pressure is taken into account, and a slowly rising level of the background pressure accounts for the weak background emission onto which the emission spikes are superimposed.)

Apart from the somewhat artificial introduction of the dead time, the kinetic model presented was restricted to mere surface processes and did not explicitly take into account effects which have to be attributed to superposition with bulk diffusion. These become particularly evident with thicker Cs layers as documented by Figs. 10 and 11. Without further extending the mathematical model, the main observations may easily be made qualitatively plausible. Due to diffusion of Cs atoms from deeper layers through an oxidized layer to the continuously oxidizing surface, the work-function minimum as well as the maximum of the exoelectron current will be reached only at higher oxygen exposures. The larger the Cs thickness, the later will this reservoir be exhausted, but the longer, on the other hand, it will take for a Cs atom to diffuse from the growing interface to the outer surface. Hence it becomes plausible why beyond a certain thickness [about 10 ML; cf. Fig. 11(b)] the total yield of exoelectrons is not increasing further. The longer a surface Cs_2O_2 has to "wait" for a Cs^0 to arrive in order to transform it into a $Cs_2O_2^*$ species, the higher the probability for the competing reaction (k_4) without electron excitation. This conclusion is corroborated by the data of Fig. 11(a) which show that even for Cs films with more than 20 ML thickness the current maximum is shifted further towards longer exposure times (i.e., oxidation still continues), although the total electron yield leveled off.

For thicker Cs layers, the variation of ϕ and I_{exo} with exposure frequently does not show a single minimum or maximum, respectively, as observed for thin layers and also reproduced by the simple kinetic model. In these cases, the emitted exoelectrons exhibit also often bimodal or even more-complex energy distributions. This indicates that the surface becomes nonuniform in a sense that patches with different local work functions (due to different oxidation stages) are coexisting on the surface. The latter effects depend sensitively on the mode of film preparation and on other parameters and are not quite reproducible experimentally. Inclusion of all these effects into a more-quantitative model does not appear reasonable.

V. CONCLUSIONS

During oxidation of thin Cs films, electrons are emitted with a total probability of the order 10^{-6} per reacting O_2 molecule. This nonadiabatic surface reaction is confined to the stage $Cs_2O_2 \rightarrow CsO_2$ and is caused by an Auger deexcitation mechanism involving a transition of electrons of the substrate near the Fermi level (as provided by Cs^0 atoms) to the empty state derived from the O_2 affinity level and located at about 2.5 eV below E_F. This affinity level will be lowered continuously with decreasing distance of the impinging O_2 molecule from the surface, and its resonance ionization upon crossing E_F can only be efficiently suppressed if no metallic states near the Fermi level are "leaking" out into the vacuum, as is the case if the surface site hit has already been transformed into Cs_2O_2. Only a small fraction of the excited electrons will, however, be able to overcome the work-function barrier—hence the rather small overall charge emitted.

A simple kinetic model based on the successive steps of oxidation of cesium is able to account qualitatively for numerous experimental observations, such as the relation between exoelectron emission, work function, and O_2 exposure, as well as for the dependence of the electron yield on temperature and O_2 pressure. The superposition of surface and bulk oxidation processes manifests itself in effects depending on film thickness, such as the observed saturation value of the totally emitted charge which is reached for films of about 10 monolayer thickness.

[1] See, for example, (a) J. R. Schrieffer, J. Vac. Sci. Technol. **13**, 335 (1976); (b) J. K. Nørskov, *ibid.* **18**, 420 (1981).
[2] T. F. Gesell, E. T. Arakawa, and T. A. Callcott, Surf. Sci. **20**, 174 (1970).
[3] T. F. Gesell and E. T. Arakawa, Surf. Sci. **33**, 419 (1972).
[4] G. C. Allen, P. M. Tucker, B. E. Hayden, and D. F. Klemperer, Surf. Sci. **102**, 207 (1981).
[5] B. McCaroll, J. Chem. Phys. **50**, 4758 (1969).
[6] B. Kasemo, Phys. Rev. Lett. **32**, 1114 (1974).
[7] B. Kasemo and L. Walldén, Surf. Sci. **53**, 393 (1975).
[8] P. I. Cohen, S. Abramowitz, and H. P. Broida, Surf. Sci. **69**, 601 (1977).
[9] L. Himmel and P. Kelly, Comments Solid State Phys. **7**, 81 (1976).
[10] T. A. Delchar, J. Appl. Phys. **38**, 2403 (1967).
[11] R. H. Prince, R. M. Lambert, and J. S. Foord, Surf. Sci. **107**, 605 (1981).
[12] M. P. Cox, J. S. Foord, R. M. Lambert, and R. H. Prince, Surf. Sci. **129**, 399 (1983).
[13] E. B. de Blasi Bourdon and R. H. Prince, Surf. Sci. **144**, 591 (1984).
[14] R. H. Prince and R. Persaud, Surf. Sci. **207**, 207 (1988).
[15] B. Kasemo, E. Törnqvist, J. K. Nørskov, and B. I. Lundqvist, Surf. Sci. **89**, 554 (1979).
[16] J. K. Nørskov, D. M. Newns, and B. I. Lundqvist, Surf. Sci. **80**, 179 (1979).
[17] A. Böttcher, R. Imbeck, A. Morgante, and G. Ertl, Phys. Rev. Lett. **65**, 2035 (1990).
[18] H. Conrad, G. Ertl, J. Küppers, W. Sesselmann, and H. Haberland, Surf. Sci. **121**, 161 (1982).
[19] G. Ertl, and J. Küppers, *Low Energy Electrons and Surface Chemistry*, 2nd ed. (VCH Verlagsgesellschaft mbH, Weinheim, 1985), Chap. 5.
[20] B. Woratschek, W. Sesselmann, J. Küppers, G. Ertl, and H. Haberland, Surf. Sci. **180**, 18 (1987).
[21] M. Skottke-Klein, A. Böttcher, R. Imbeck, S. Kennou, A. Morgante, and G. Ertl, Thin Solid Films (in press).
[22] J. Hrbek, Surf. Sci. **164**, 139 (1985); T. K. Sham and J. Hrbek, J. Chem. Phys. **89**, 1188 (1988).
[23] H. Bludau, H. Over, M. Skottke-Klein, W. Moritz, and G. Ertl (unpublished).
[24] B. Woratschek, W. Sesselmann, J. Küppers, G. Ertl, and H. Haberland, J. Chem. Phys. **86**, 2411 (1987).
[25] J. Lee, C. Hanrahan, J. Arias, F. Bozso, R. M. Martin, and H. Metiu, Phys. Rev. Lett. **54**, 1440 (1985); B. Woratschek, W. Sesselmann, J. Küppers, G. Ertl, and H. Haberland, *ibid.* **55**, 611 (1985).
[26] B. Woratschek, G. Ertl, J. Küppers, W. Sesselmann, and H. Haberland, Phys. Rev. Lett. **57**, 1484 (1986).
[27] *Gmelins Handbuch der Anorgan. Chemie, 8. Aufl., Bd. 25 Caesium* (Verlag Chemie, Berlin, 1938), pp. 112 and 113.
[28] G. Ebbinghaus and A. Simon, Chem. Phys. **43**, 117 (1980).
[29] C. Y. Su, I. Lindau, P. W. Chye, S.-J. Oh, and W. E. Spicer, J. Electron Spectrosc. **31**, 221 (1983).
[30] A. Böttcher, R. Grobecker, R. Imbeck, and G. Ertl (unpublished).